Planetary and Space Science 58 (2010) 459–471

Contents lists available at ScienceDirect

Planetary and Space Science

journal homepage: www.elsevier.com/locate/pss

Yardangs in terrestrial ignimbrites: Synergistic remote and field observations on Earth with applications to Mars

de Silva S.L.[a,*], Bailey J.E.[b], Mandt K.E.[c], Viramonte J.M.[d]

[a] Department of Geosciences, Oregon State University, Wilkinson Hall 104, Corvallis, OR 97331, USA
[b] Alaska Volcano Observatory, University of Alaska, Fairbanks, AK 99775, USA
[c] Southwest Research Institute, 6220 Culebra Rd, San Antonio, TX 78238, USA
[d] Instituto GEONORTE, Universidad Nacional de Salta, Av. Bolivia 5150, 4400 Salta, Argentina

ARTICLE INFO

Article history:
Received 14 April 2009
Received in revised form
29 September 2009
Accepted 5 October 2009
Available online 17 October 2009

Keywords:
Yardangs
Ignimbrites
Andes
Mars analog

ABSTRACT

The conditions of formation and the form of yardangs in ignimbrites in the Central Andes of Chile, Bolivia, and Argentina may be the most convincing terrestrial analog to the processes and lithology that produce the extensive yardangs of the Medusae Fossae Formation (MFF) of Mars. Through remote and field study of yardang morphologies in the Central Andes we highlight the role that variable material properties of the host lithology plays in their final form. Here, ignimbrites typically show two main facies: an indurated and jointed facies, and a weakly to poorly indurated, ash- and pumice-rich facies. Both facies are vertically arranged in large (erupted volume >100's of km^3) ignimbrites resulting in a resistant capping layer, while smaller (10's of km^3) ignimbrites are made predominantly of the weakly indurated facies. The two facies have quite different mechanical properties; the indurated facies behaves as strong rock, fails by block collapse and supports steep/vertical cliffs, while the non-indurated facies is more easily eroded and forms gentle slopes and manifests as more subdued erosional forms. In response to aeolian action, the presence of an upper indurated facies results in large, elongate, high aspect ratio (1:20–1:40) megayardangs that form tall (100 m), thin ridges with steep to vertical walls. These are built on a broad apron of the weakly indurated facies with abundant fallen blocks from the upper indurated facies. These terrestrial megayardangs appear to be analogous to megayardangs with associated block fields seen on Mars. Smaller-volume, weakly indurated ignimbrites are sculpted into smaller, stubbier forms with aspect ratios of 1:5–1:10 and heights rarely exceeding 10 m. Excavation of a windward basal moat suggests an erosional progression like that seen in incipient yardangs on Mars. Excavation rates of 0.007–0.003 cm/year are calculated for the weakly indurated ignimbrites. While a persistent strong unidirectional wind is the dominant parameter controlling yardang formation and orientation, a role for flow separation and vorticity is also suggested by our observations at both yardang types. While the indurated facies is commonly pervasively jointed, jointing is of secondary importance in controlling yardang orientation. Serrated margins, a common feature on Mars, result from oblique intersections of jointing with yardang flanks or scarps of ignimbrite. The processes of yardang formation we describe from ignimbrites from the Central Andes are not necessarily specific to ignimbrites, but do connote that degree and distribution of induration is a major control in yardang formation and this has implications for the lithology of the MFF on Mars.

© 2009 Elsevier Ltd. All rights reserved.

1. Introduction

A perennial challenge to terrestrial and planetary geologists is to understand remotely sensed features in terms of process and properties of the host lithologies. Among the geomorphic features common to Earth and Mars are yardangs (Blackwelder, 1934; Ward, 1979)—remnant wind-eroded aerodynamic ridges and associated minor variants (Fig. 1). The final form and texture of wind-eroded forms are strongly dependent on rock structure (massive, layered, jointed) and material properties (hardness, homogeneity, grainsize, and cohesion) because these properties control the erosional effectiveness of the wind (Breed et al., 1989) and the character of the ridges and slopes of the resulting forms (Selby et al., 1988). On Earth, extensive yardang fields are found in a variety of deposits ranging from lake deposits (Iran, US), sandstones (Peru), and ignimbrites (primary volcaniclastic rocks) and lava flows (Andes), among others, as summarized in Table 1.

* Corresponding author. Tel.: +1 541 7371212.
E-mail addresses: desilvas@geo.oregonstate.edu (S.L. de Silva).
jbailey@gi.alaska.edu (J.E Bailey), kmandt@swri.edu (K.E Mandt).

0032-0633/$ - see front matter © 2009 Elsevier Ltd. All rights reserved.
doi:10.1016/j.pss.2009.10.002

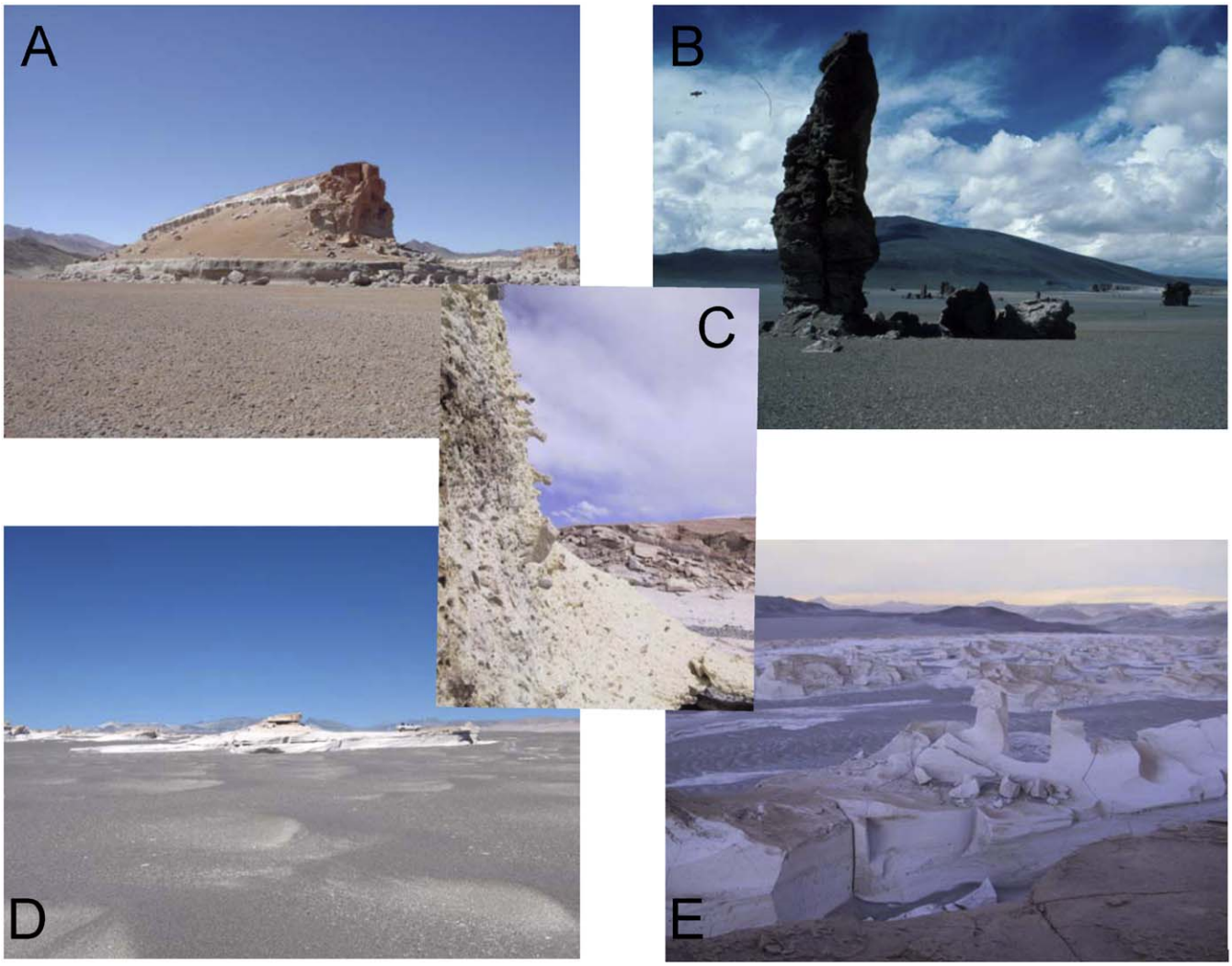

Fig. 1. Aeolian erosional forms in ignimbrites in the Central Andes. (A) 40 m high, 300 m long megayardang in indurated ~2 Ma Cerro Galan ignimbrite, NW Argentina. (B) 30 m high pillar-like hoodoo remnant of the 3.8 Ma Tara ignimbrite in N. Chile. Remnants of the ignimbrite sheet can be seen as other hoodoos or demoiselles throughout this area. (C) Spongy and fluted "modified tafoni" textured block (face is ~1.5 m) showing detail of the abraded surface of weakly indurated ignimbrite. (D) 10 m high, 80 m long mature yardang in the 70 ka weakly indurated Campo de Piedra Pomez ignimbrite NW Argentina. Note vehicle for scale. This is one of the largest yardangs in these weakly indurated ignimbrites. (E) Various hoodoo and demoiselle forms characterize this area of the Campo Piedra Pomez. The faces are strongly fluted and show strong concavity. Height of largest hoodoo in the foreground is 8 m above the ground (rippled area). Meter scale blocks attest to secondary sculpting of ignmbrite through collapse.

This compilation shows that although there is wide-ranging variability in yardang morphology, there is a strong relationship between aspect ratio, height, and slopes. These are largely a function of the degree of induration (hardening) of the deposits (Blackwelder, 1934), with poorly indurated material forming small, stubby yardangs, and indurated deposits supporting long, high, steep-sided yardangs. Of all the terrestrial yardang fields compiled by us (Table 1), the erosional pattern is most regionally pervasive where ignimbrites are the host lithology.

On Mars, the nature of the host lithology of ubiquitous yardangs there has been the subject of considerable debate, the resolution of which may rest on observations from appropriate terrestrial analogs until these features can be studied directly. Through remote and field study of yardang morphologies in extensive regional ignimbrite sheets in the Central Andes, we have compiled a set of empirical data on the process of yardang formation and the role that the variable material properties of the host lithology plays in their final form. In this contribution we present these observations. The reader is first given some background to Medusae Fossae Formation on Mars and the yardangs found therein. The focus is then shifted to the Central Andes and its ignimbrites, their material properties and the processes of yardang formation there. We show that the processes of yardang formation in ignimbrites with different material properties are analogous to those inferred to have formed yardangs on Mars. Our observations also emphasize the importance of the degree and distributon of induration (hardness, coherence, resistance to erosion) of the host lithology in controlling the processes of yardang formation and their final morphology.

2. Yardangs on Mars

Among the most obvious features on the surface of Mars are the abundant yardangs in the Medusae Fossae Formation (MFF) on Mars (Ward, 1979), interpreted to be the result of the mildly indurated nature of the MFF lithology and the presence of strong unidirectional winds (Schultz and Lutz, 1988; Scott and Tanaka, 1982). One of the most prominent formations on Mars, the MFF is a deposit located along the equator stretching between 240° and 170°E. It is commonly termed enigmatic because its origin has

Table 1
Characteristics of yardangs on Earth and Mars (updated from Mandt et al. 2008).

Location	Lithology	Yardang characteristics
Iran, Lut Desert[a]	Silty clays, gypsiferous sands. moderately indurated	10's of km long. 60–80 m tall
Peru, Pisco Formation[b]	Marine sediments	
China, Lop Nor[a,c]	Lake beds	100's of meters long, 20 m high Aspect ratio up to 1:10
Rogers Lake, CA, USA[d]	Gravel, sand, silt, and clay moderately consolidated	1:5
Egypt, Western Desert[c,e]	Silicified limestone, lake beds. Chalk	10–100 m long, 2–5 m tall.
Chad[e]	Indurated Sandstone	20–30 km long, 1 km wide. Aspect ratio 1:20–1:30. Spacing 500 m–2 km
Argentina—Payun Matru[f]	Ignimbrites and lavas	2–10 km long; Lavas result in broad troughs. Ignimbrites – yardangs
N. Saudi Arabia[c]	Cambrian sandstone	40 m high, hundreds of meters long
Namibia[c]	Igneous and metamorphic basement	8–10 km long. Spacing 300–350 m. Aspect ratios up to 1:20
Chile, Bolivia, Argentina—Central Andes[g]	Ignimbrites. variably indurated, welded	Aspect ratio. Indurated 1:20–1:40. Non-indurated: 1:5–1:10. Up to 100 m tall (indurated). $<$ m tall (non-indurated). Slopes: vertical to steep (indurated). Length 10's of meters (non-indurated) to kilometers (indurated)
Mars–MFF[h,i]	Medusae Fossae Formation	Slopes: vertical to steep. Height: $>$ 100 m (range 5–700 m). Aspect ratio 1:5 minimum to 1:20–1:50

[a] McCauley et al. (1977b).
[b] McCauley (1973).
[c] Goudie (2007).
[d] Ward and Greeley (1984).
[e] Breed et al. (1989).
[f] Inbar and Risso (2001).
[g] Bailey et al. (2007)
[h] Ward (1979).
[i] Mandt et al. (2008).

been debated for decades. The MFF is located in the Amazonis Planitia region and lies between two major volcanic centers; Tharsis and Elysium (Fig. 2A). In all places where they are in contact, the southern portion of the MFF overlies the dichotomy boundary, a great circle inclined 28° to the equator that divides the northern lowlands from the southern, cratered highlands (Greeley and Guest, 1987). The MFF is considered to be one of the youngest deposits on Mars based on stratigraphic relationships (Scott and Tanaka,1986; Greeley and Guest,1987; Head and Kreslavsky, 2004; Hynek et al., 2003). A wide variety of hypotheses has been proposed for the geologic origin of the MFF: ignimbrites (Scott and Tanaka, 1982; Mandt et al., 2008, 2009), aeolian deposits (Greeley and Guest, 1987), paleopolar deposits (Schultz and Lutz, 1988), exhumed fault rocks (Forsythe and Zimbelman, 1988), carbonate platform (Parker, 1991), rafted pumice deposits (Mouginis-Mark, 1993), lacustrine deposits (Malin and Edgett, 2000), ash fall tuff (Tanaka, 2000; Bradley et al., 2002; Hynek et al., 2003), and deposits associated with a subsurface aquifer (Nussbaumer, 2005).

Yardangs in the MFF occur across the extent of the deposit and within various members at different elevations. Ward (1979) observed that yardangs in the MFF on Mars were considerably larger and more elongate (aspect ratios up to 50:1) than mature terrestrial yardangs (ideal aspect ratio 4:1; Ward and Greeley, 1984). He suggested that the size, slopes, and forms of Martian yardangs implied an indurated lithology that weathers to a granular substrate. The other pervasive lithologic property attributed to the MFF lithology is jointing, which Bradley et al. (2002) attributed to cooling and compaction (see also Scott and Tanaka, 1982). Taking advantage of the growing library of high resoution data for Mars, Mandt et al. (2008) measured detailed morphometric parameters for the MFF yardangs. They showed that the height and slope of megayardangs are on average 75–80°, that they range in height from 5 to 700 m, with the majority being over 100 m tall, and that their widths range from one to five kilometers. Based on these measurements, Mandt et al. (2008) inferred material properties and argued that the form of the MFF yardangs require a lithology that is indurated in its upper parts and more friable in its lower portions. They proposed that the lithology of the MFF is largely ignimbrites.

While wind erosion is known to be the primary process of yardang formation (Blackwelder, 1934; Breed et al., 1989), our continued work on the MFF yardangs has revealed further details of the processes and two predominant mechanisms of yardang formation in the MFF have been identified.

(1) Undercutting and resulting block collapse of a strongly indurated upper zone (Mandt et al., 2008). This is supported by recent high resolution HiRiSE data that show block fields surrounding megayardangs. (Fig. 2C).
(2) An erosional progression from v-shaped depressions to fully fledged yardangs (Fig. 2D) as described bv Mandt et al. (2009).

The first case results in the megayardangs, the second in smaller features. We find analogies to these processes and forms in the ignimbrites of the Central Andes and describe these below.

3. Yardangs in ignimbrites in the Central Andes

Ignimbrites are primary volcaniclastic deposits left by pyroclastic flows in which pumice (blocks of vesiculated magma) is contained in a matrix of fine ash, crystals, and lithic fragments. For a full review of ignimbrites the reader is referred to Ross and Smith (1961), Cas and Wright (1992) and Branney and Kokelaar (2002). What follows is a précis of the key transport and depositional processes that are relevant to understanding the variable properties of ignimbrites.

Pyroclastic flows form during the climactic phase of the most explosive volcanic eruptions on earth, often associated with caldera formation, when violent ground-hugging flows of ash, gas, and pumice with internal temperatures as high as 700 °C, move at velocities $>$100 km/hr away from the eruption source. Depending on the volume of material erupted, ignimbrites may inundate the local and regional topography, leaving a flat-topped smoothed surface sheet of variably friable material. The largest ignimbrites on Earth, such as those that will be described here, can cover many 1000s of square kilometers and extend 100s of kilometers in all directions from their source volcanoes. The high temperature of the flows and abundance of hot gas, from breakage of pumice and ingestion and heating of ambient air, result in significant post-depositional diagenesis as the deposits cool and trapped hot gases gradually percolate upwards and escape. The most common diagenetic effect is the development of a profile where the upper parts of the deposit are indurated through cementation and sintering of the matrix ash, while the lower portions remain poorly to weakly indurated (Ross and Smith, 1961, Roever, 1966; de Silva, 1989b). In the upper indurated zone, thermal and mechanical contraction often produces pervasive

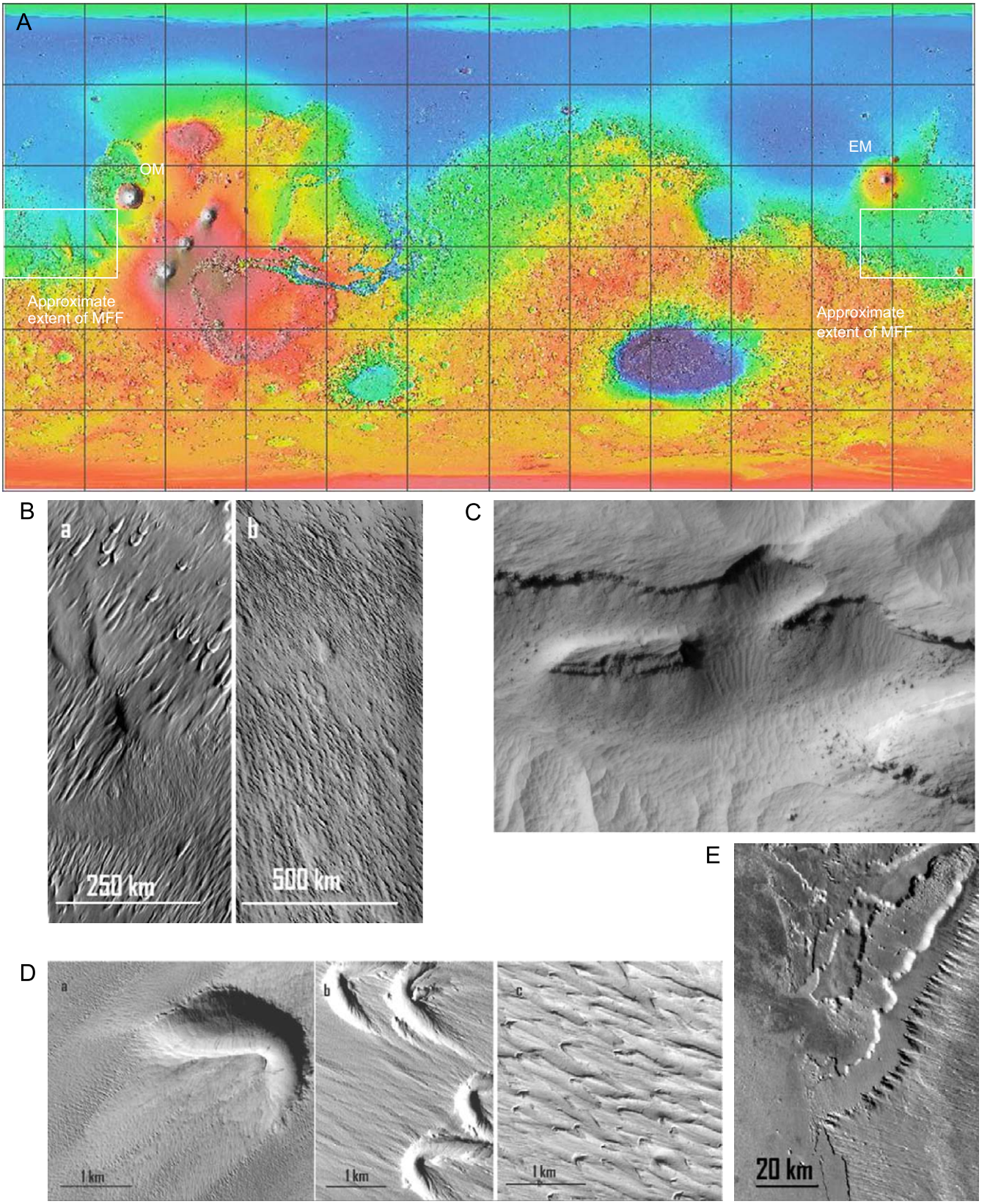

Fig. 2. The Medusae Fossae Formation, Mars, yardangs therein, and associated features. (A) Whole planet topography of Mars showing the distribution of the MFF straddling the dichotomy boundary in an equatorial belt from Olympus Mons (OM) to Elysium Mons (EM). (MOLA data, NASA and USGS). (B) THEMIS images showing features of megayardangs in the MFF. (a) THEMIS daytime IR I10241007 showing progression from v-shaped depressions to curvilinear yardangs (see Mandt et al., 2009). (b) THEMIS visible V01054003 showing erosional progression from feathered scarps (bottom of image) to curvilinear yardangs. (C) Portion of HiRISE image PSP_001448_1735 revealing the layered and indurated nature of the MFF material. Note the block fields at the base of the cliffs and yardangs and development of peripehral transvere aeolian ridges (TARs). Yardang in center is ~1 km in length. (D) Erosional progression from v-shaped depressions to curvilinear yardangs. (a) MOC e1000390 illuminated from the top of the image showing a single v-shaped depression. (b) MOC m0700371 illuminated from the right, showing a cluster of v-shaped depressions. (c) MOC m2101904 illuminated from the right, showing yardangs with remnant v-shaped depressions at their tips. Note the difference in scale in B and C. (E) infrared I17167016 showing a 3 km-high serrated scarp.

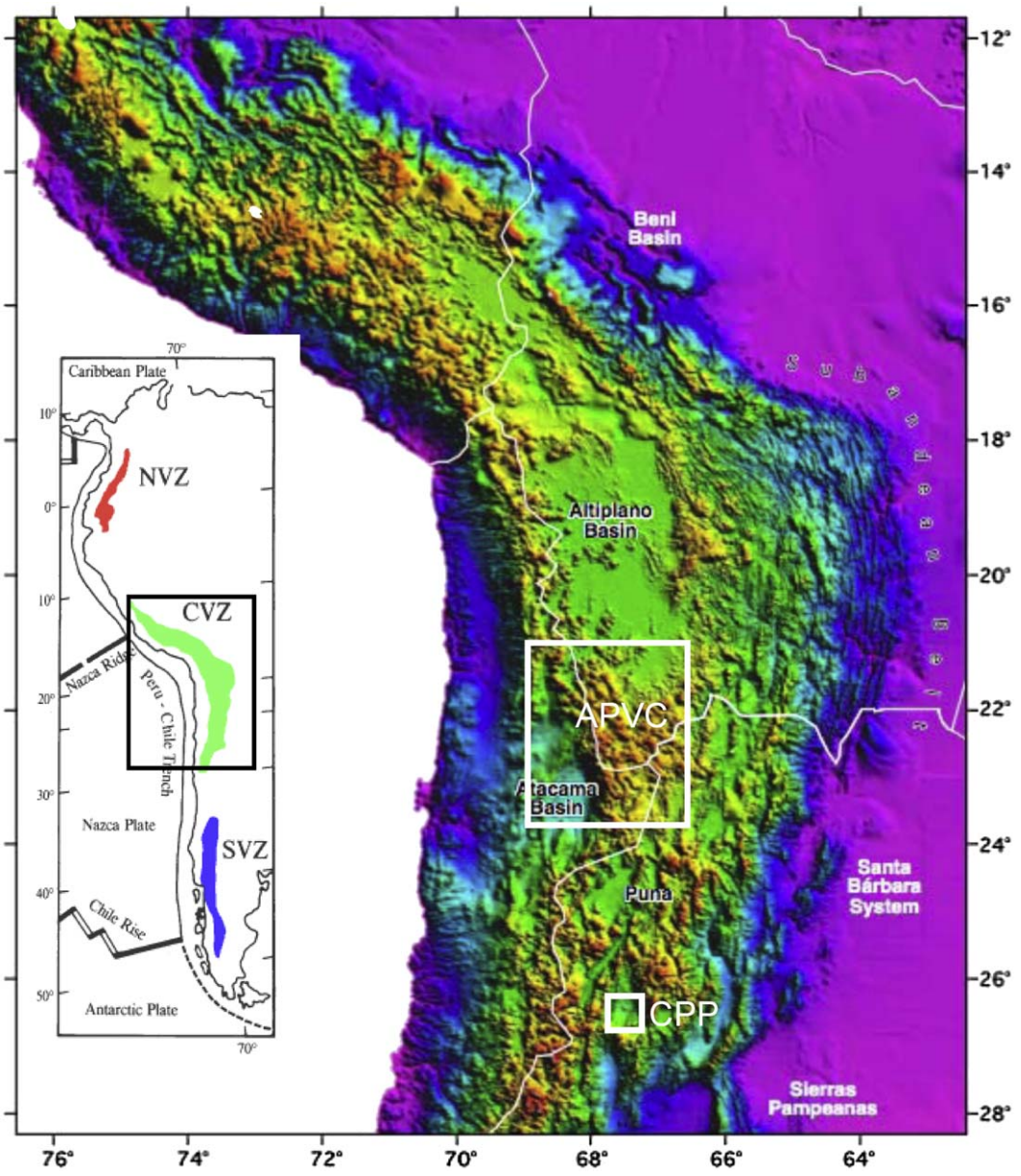

Fig. 3. Physiography of the Central Andes in shaded relief, based on the 1-km DEM of the Defense Mapping Agency (adapted from Allmendingeret al., 1997). The Altiplano–Puna plateau is located down the center of the mountain chain. The location of the two study areas in this paper are shown. The Altiplano–Puna Volcanic Complex (APVC) is located at the transition between the Altiplano and the Puna, and the Campo Piedra Pomez (CPP) towards the southern end of the Puna. Elevations range from sea level (magenta) to >6000 m (red). Base elevations in the Puna are about 4200 m while in the Altiplano they are 3800 m. Inset shows volcanic and tectonic segmentation of the Andean margin. The area of interest is the Central Volcanic Zone (CVZ) of the Central Andes (box).

jointing, commonly columnar, throughout the upper zone. It should be noted that *induration* is a chemical and thermal hardening process that does not involve flattening, and is different from *welding*, which does involve flattening (due to either load or volatile resorbtion), loss of pore space and densification of the ignimbrite. The zone of maximum welding does not have to correspond to the zone of chemical induration.

The result of the processes above is that large volume (>100's of km^3 with areas $\gg 1000$s of km^2) ignimbrites typically show two main facies: an upper commonly massive, indurated and jointed facies, and a lower weakly to poorly indurated, ash- and pumice-rich facies that may show internal layering but can also be massive. These two facies can have a welding profile superimposed on them, but this is not typical and is often only local in occurrence. The two main facies may occur individually, may be locally vertically associated, or grade into each other laterally (the result of heat loss by the pyroclastic flow as it travels). The two facies have quite different mechanical properties; the upper facies behaves as strong rock with high compressive strength, fails by block collapse, and supports steep/vertical cliffs, whereas the lower facies is weaker and acts like a strong soil and only supports gentle slopes (Selby et al., 1988, Crown et al., 1989).

Smaller-volume ignimbrites (10's of km^3 and areas of 100's of km^2) tend to largely display the weaker poorly indurated facies with only minor or local development of induration–this is due to a complex relationship between volumes and compositions erupted, degree of inflation of the flows, and the resulting differences in thermal histories of the flows. Large-volume

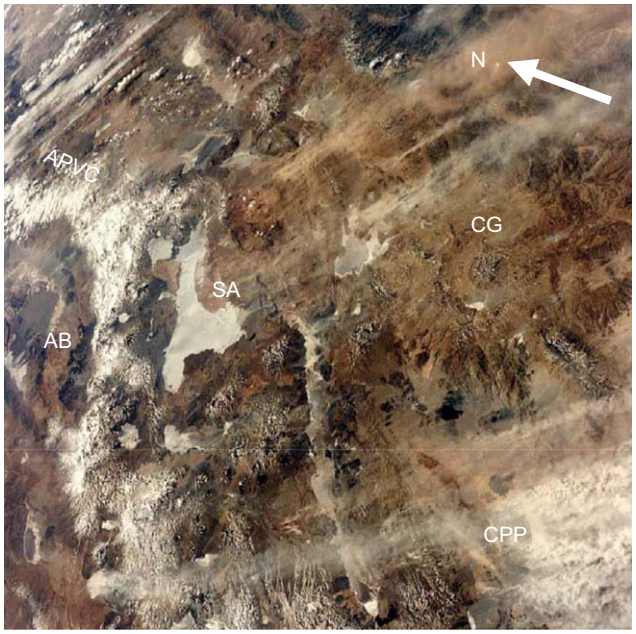

Fig. 4. Oblique space-shuttle photograph (S-08-31-0858) showing NW-SE trending plumes (streaks) of dust resulting from the ubiquitous aeolian erosion in a swath of the Central Andean Puna from about 22 °S (top left) to 26.5 °S (Bottom right). Tan plumes are ash plumes from erosion of ignimbrites, while white plumes are either of ash or salt. AB- Atacama Basin, SA - Salar de Arizaro, CG - Cerro Galan, and the two study areas for this paper the APVC - Altiplano Puna Volcanic Complex; and the CPP - Campo Piedra Pomez. Arrow indicates north.

ignimbrites tend to be intermediate in composition and erupt hotter magmas in lower and denser eruptive columns that promote heat retention and post-emplacement induration (e.g. de Silva et al., 2006). The key is that the variable material properties of ignimbrites result in quite different responses to erosional agents. We now focus on aeolian erosion of ignimbrites in the Central Andes and the insights we have gained about the processes of yardang formation.

3.1. The Altiplano–Puna plateau—an analog aeolian laboratory for Mars

The Altiplano–Puna of the Andes is the second highest (4000 m average a.s.l) plateau on Earth. Located between 18 and 28 °S, it extends for over 1500 km N-S, and 300 km E-W (Fig. 3). Peaks above the plateau, predominantly volcanic, rise over 6000 m. Large-scale circulation in this region produces strong, consistent NW-SE winds throughout the region. Since the Andes mountains act as a large meriodinal barrier to low level moisture transport, the Altiplano–Puna plateau receives little precipitation (rain shadow), resulting in a climate that varies from semi- to a hyper-arid with latitude and altitude. This climate has persisted for several millions of years (Greene, 1995; Gaupp et al., 1999; Hartley and Guillermo Chong, 2002). Here, the role of the wind in the geomorphic expression of the surface is clear (Fig. 4) with abundant modern landforms such as sand dunes (barchan, parabolic, and linear), windstreaks (salt and ash), and paleo- and modern landforms including prominent yardangs (Greene, 1995, Bailey et al., 2007). These are best developed in the regionally extensive ignimbrite sheets that dominate the surface of the plateau (Bailey et al., 2007, de Silva et al., 2008).

It has long been recognized that aeolian features in this part of the Central Andes have a dominant NW-SE trend (e.g. Greene, 1995) and Bailey et al. (2007) have shown that yardangs in the APVC are one end member of a spectrum of erosional forms that are produced by fluvial and aeolian erosion (Fig. 5). On remotely sensed images, aeolian erosion dominated features can be identified by their linear nature and alignment in a coherent, cross-slope direction. An important role for the pervasive jointing characterisitic of large ignimbrites in the orientation of linear channel and ridge topography in the APVC was suggested by early work (Guest, 1969; de Silva, 1989a) with possible influence of the NW-SE regional tectonic grain. However, it is now clear that no correlation exists between regional faulting, and the location and orientation of surface features (Fig. 6). It appears that some joint planes have encouraged development of wind-derived features but as we will show below, these are only a contributing factor to yardang formation. The primary factor that controls the general NW-SE direction of aeolian features in the Andes is the wind (Greene, 1995, Inbar and Risso, 2001, Bailey et al., 2007). Since yardangs are pervasive in terrains of different ages, this long term coherence in the alignment suggests strong unidirectional winds have been in operation at least for the last 2 Ma based on superposition relationships (Greene, 1995). It should be noted that at the 4000 m average altitude of the plateau atmospheric pressure is only about 0.65 bars, making the pervasive aeolian imprint in this region all the more impressive.

We now turn our focus to our two study areas in this vast plateau. Between 22° and 24 °S straddling the border of Chile, Bolivia, and Argentina is the 10–0.09 Ma *Altiplano Puna Volcanic Complex* (APVC), one of the largest ignimbrite provinces on the planet (de Silva et al., 1989a,b; de Silva et al., 2006). The second area is the *Campo Piedra Pomez* (CPP), a small volume ignimbrite field formed about 70–13 ka (Arnosio et al., 2005; *de Silva* et al. unpublished ^{40}Ar-^{39}Ar data) located between 26 and 27 °S in the Catamarca province of Argentina.

3.2. Yardang formation in Central Andean ignimbrites

In the APVC, four of the most extensive units were erupted about ~4 Ma; these are the 4.09 Ma Puripicar, the ~4.0–3.91 Ma Toconao-Atana ignimbrite pair, and the 3.84 Ma Tara ignimbrite. Details of these units can be found in de Silva (1989b) and Bailey et al. (2007). These ignimbrites are large-volume, regionally extensive units that locally can form windward cliffs 10's to 100 m high. These cliffs reveal an indurated, pervasively jointed upper facies and a lower weakly indurated facies. This profile results in large, elongate, high aspect ratio (20:1–40:1) yardangs, that form tall (100 m), thin ridges with steep to vertical walls (Fig. 7). These *megayardangs* (cf. Goudie, 2007) demonstrate the importance of differential induration and mechanical weathering in producing tall, steep-sided, megayardangs with broad shallow-sloped bases (Fig. 8).

In the Campo Piedra Pomez (Fig. 9), a small volume rhyolitic ignimbrite that erupted from the Cerro Blanco Caldera ~70 ka typically forms cliffs < 10 m tall. These weakly indurated ignimbrites are carved into stubby and chaotic yardangs, demoiselles (hoodoos), with aspect ratios of 5:1–10:1 and heights rarely exceeding 10 m (Fig. 1, D, E and Fig. 10).

In many locations, serrated margins quite like those in the MFF (Fig. 2E) result from oblique intersections of jointing and yardangs or scarps of ignimbrite sheets (Fig. 7D). The jointing does not control yardang orientation, but can assist in the sculpting process and affect the final form. Thus, yardangs in ignimbrites with well developed jointing clearly demonstrate no correlation between prominent joint direction and yardang orientation supporting the assertion that a persistent, strong unidirectional wind is the dominant parameter controlling yardang orientation.

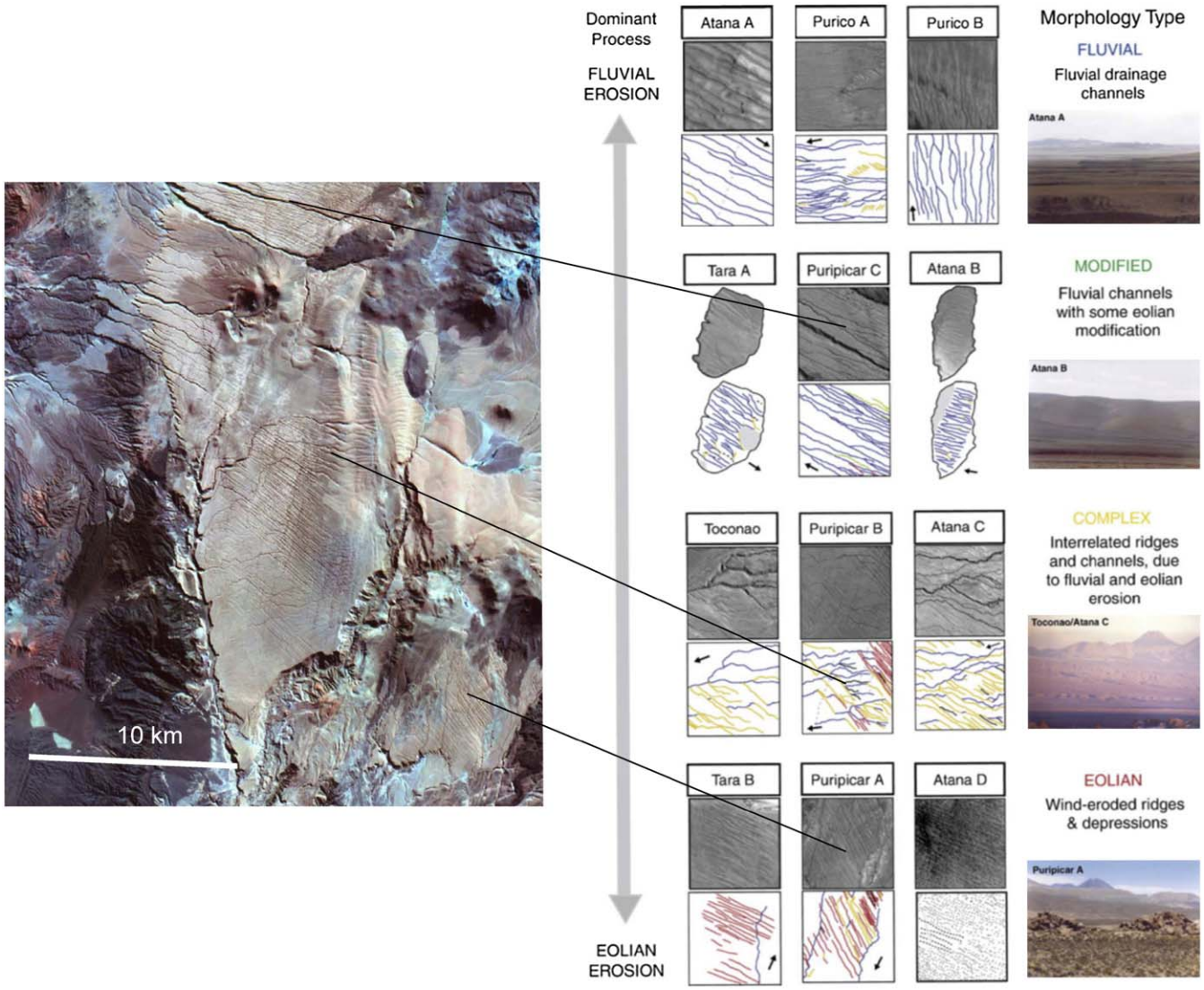

Fig. 5. Spectrum of erosional forms that are produced by fluvial and aeolian erosion in the APVC. (A) The interplay between these agents is well illustrated in the 4.09 Ma Puripicar ignimbrite plateau in northern Chile. The image is a Landsat FCC using Bands 7,4, and 2 in RGB. North to the top. (B) Classification of surface morphologies showing the dominant erosional processes. Photos of example sites from each category are shown on the right (after Bailey et al., 2007).

3.3. *Formation of megayardangs in indurated ignimbrites*

The megayardangs in the Central Andes clearly provide evidence of the importance of a strong indurated upper layer to the ignimbrites. The abundance of large fallen blocks of indurated ignimbrite from the upper facies strongly implicates block collapse. In combination these two observations suggest that the yardang was sculpted as the upper indurated layer is undercut by removal of the weaker lower facies of the ignimbrite (Fig. 8). This appears to be the primary mechanism of megayardang development in these indurated ignimbrites and appears to have direct analogy to martian megayardangs like those in Fig. 2C.

The process is inferred to initiate by mechanical and chemical weathering along joints or re-entrants in a coherent ignimbrite sheet to expose the weaker lower facies. These re-entrants might be clefts in an originally lobate margin, incipient fluvial channels guided by primary waves on the upper surface of the ignimbrite (e.g. Richards and Villeneuve, 2002), or fumarolic mounds in the upper part of the sheet. Once erosion is initiated the base is exposed to persistent abrasion by saltating impactors–abundant quartz is available as an ablator. A distinct fluting and grooved texture (referred to as "tafoni" by Bailey et al. (2007) because it accentuates primary tafoni texture produced by alteration and weathering of the ignimbrite) is often seen in the lower weak facies and on many fallen blocks. This strongly implicates abrasion in the saltation zone. This texture is not seen in the upper indurated layers that typically show clean, vertical faces. We interpret this difference to implicate two different processes of erosion of the lower and upper facies. The softer base of the indurated cliffs is eroded through saltation impact and the debris is deflated away. Evidence of fluting and grooving in the upper limits of the weak zone well above the ground level attests to lowering of the base level over time. The removal of the weaker basal layers results in undercutting of the upper cliff-former and these jointed and indurated cliffs collapse or peel away in huge blocks. These fallen blocks themselves get gradually abraded and deflated away once they fall down into the saltation zone. Remnants of these blocks produce the prominent block fields surrounding the megayardangs and many are strongly fluted and grooved in situ. Haphazard orientation of fluting and grooving on the blocks suggests complex wind flow locally. Deflated material is deposited in lateral ripple fields along the flanks of the

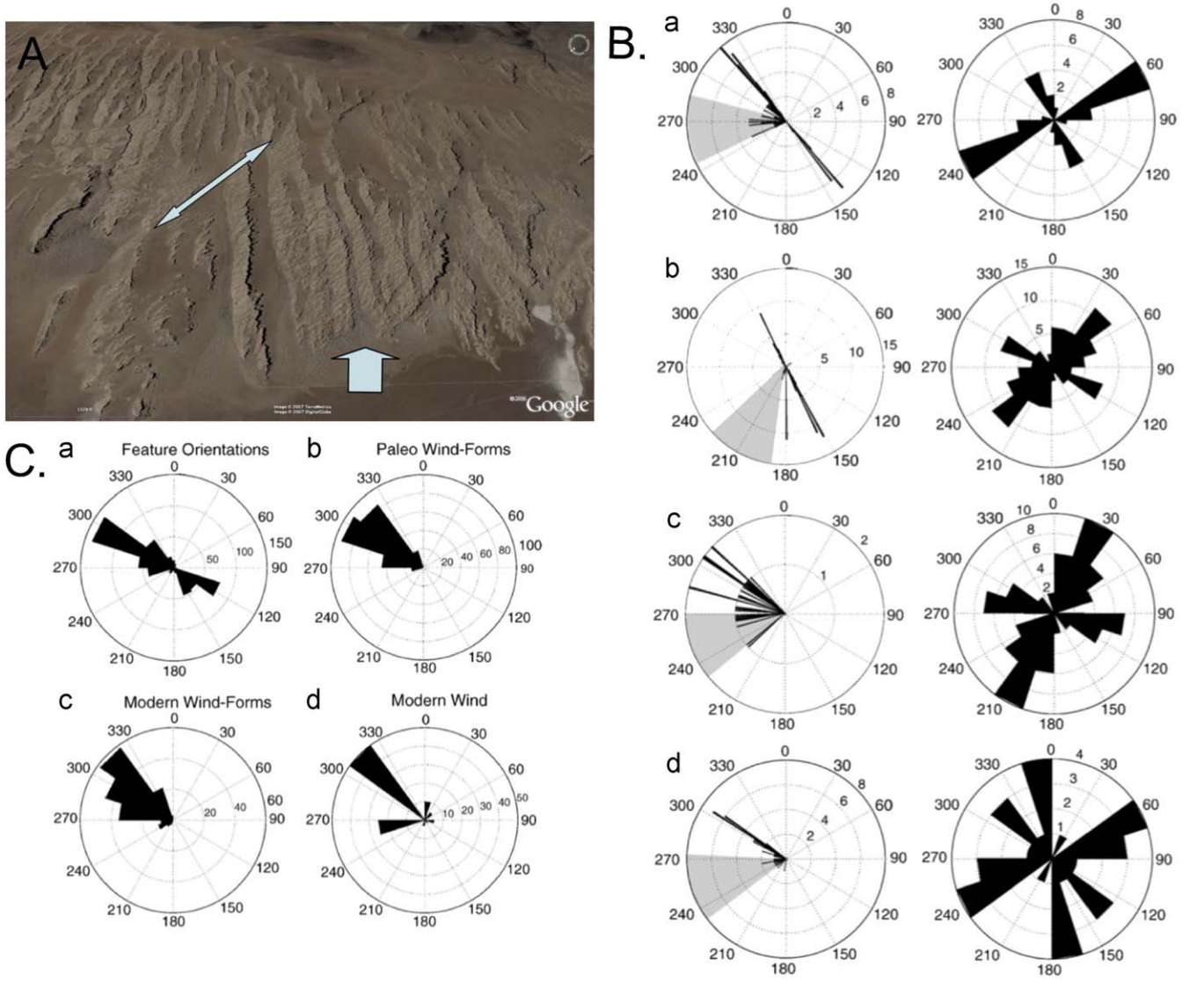

Fig. 6. While the indurated facies of ignimbrites is commonly pervasively jointed, this is of secondary importance and a persistent strong unidirectional wind is the dominant parameter controlling yardang orientation. (A) Aeolian erosion and yardang formation in the indurated 5.6 Ma Chuhuilla ignimbrite in SW Bolivia. North is to the bottom left, prevailing wind is from NW to SE (large arrow). The longest of these ridges is about 2 km long and aspect ratios of 1:20 are common here. Note the discordance between pervasive jointing (small arrow) and wind direction and the resulting serrated margins and rhomboid blocks. Oblique view from west to east. Google Earth image used with permission. (B) Comparison of feature orientation (left) with the orientations of cooling joints (right) at four sites measured in the field (after Bailey et al., 2007): (a) Puripicar B, (b) Puripicar A, (c) Toconao, and (d) Atana C. Shaded areas indicate those features that are defined as along-slope; unshaded as cross-slope. (C) Evidence for modern and paleo wind directions around La Pacana Caldera (after Bailey et al., 2007). (a) Cumulative orientations of studied surface features. (b) Modern wind direction-based erosional structures in Puripicar Ignimbrite (Greene, 1995). (c) Modern wind directions based erosional structures in Puripicar Ignimbrite (Greene, 1995). (d) Survey of current atmospheric circulation conditions (Das et al., 1998). (B and C from Bailey et al., 2007).

yardangs. Combined with the arcuate and locally haphazard fluting and grooving, we hypothesize that these ripples implicate local vortices that develop as the primary wind separates around the yardang and is further interfered with by the fallen blocks and by negative flow (e.g. Whitney, 1983). Horsetail vortices may have formed along the flanks (e.g. Greeley and Iverson, 1985) and may account for the ripple spacing. This could be tested through field experiments and more detailed mapping of the ripples, flutes and grooves.

3.4. *Yardang formation in weak ignimbrites*

Most of the yardang forms in the poorly indurated ignimbrites of the Campo Piedra Pomez (CPP) we focus on here are immature or incipient in our interpretation. This is based on the fact that we see a progression from incipient to mature forms like that shown in Fig. 1D. The few mature yardangs we examined clearly show the characteristic elongate streamlined tapered forms, with concave-convex facial associations, fluting, and keeled back slopes. Our focus was to understand the initiation and early development of yardangs as an analog to the martian incipient yardangs and v-shaped depressions we have previously posited (Fig. 2D).

The majority of the forms shown in Fig. 9 are stubby, with blunt prows and convex ‘‘whalebacks’’. Of particular note are the windward ‘‘moats’’ at the base of the prow. These are not delation hollows as they involve excavation of the bedrock. We observe that the yardang is anchored at a resistant node formed by local induration by escaping gases (a large fumarolic mound; Fig. 10C). The prows of these yardangs in the CPP are arranged in curvilinear arrays that follow alteration-rich fractures or joints (Figs. 9, 10B). Based on these observations we suggest a progression of yardang formation (Fig. 11) where a vapour-phase indurated knob of ignimbrite promotes local flow separation and vorticity. Saltating

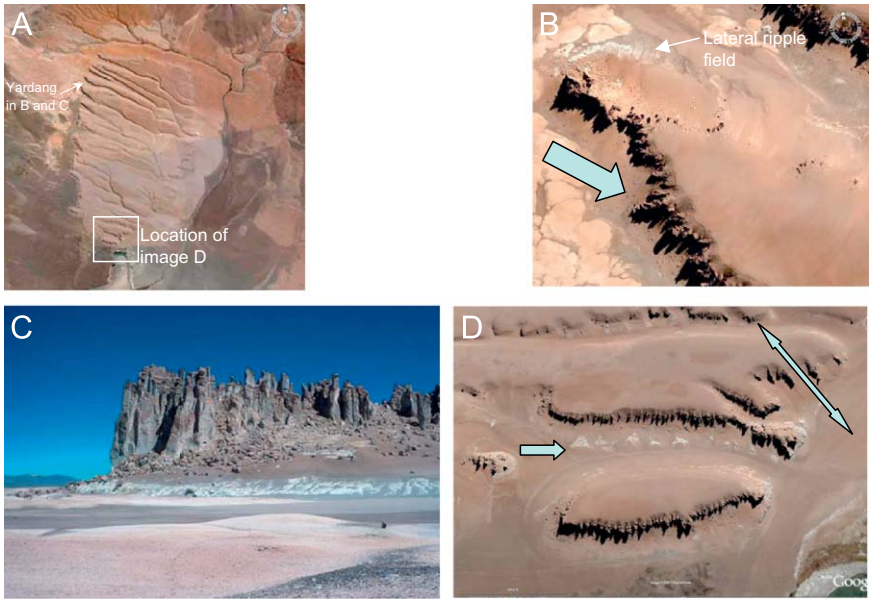

Fig. 7. Aerial and field views of megayardangs in the 3.8 Ma Tara ignimbrite of the APVC of northern Chile. (A–C) show different scales of view of the same yardang (arrow in A shows its context). Large blue arrow in B shows the prevailing wind direction. (C) shows field image of the 100 m tall megayardang clearly exhibiting the two different facies. The lower weak facies forms the white sloping apron to the upper pervasively indurated and jointed cliff-former. Note the extensive block field on the apron attesting to collapse and recession of the cliff. Many of these blocks now show the fluted and grooved modified tafoni texture of wind abrasion. These yardangs demonstrate the importance of differential induration and mechanical weathering in producing tall, steep-sided, megayardangs with broad shallow-sloped bases surrounded by block fields. (D) Serrated edges in mature yardangs (aspect ratio 1:4) in the 3.8 Ma Tara ignimbrite produced by pervasive jointing (double headed arrow) oblique to wind direction (from left). The yardangs have grown by deepening and widening ancestral fluvial channels. Image center. 22°58'24.01S 67°18'12.74W. Google Earth images used with permission.

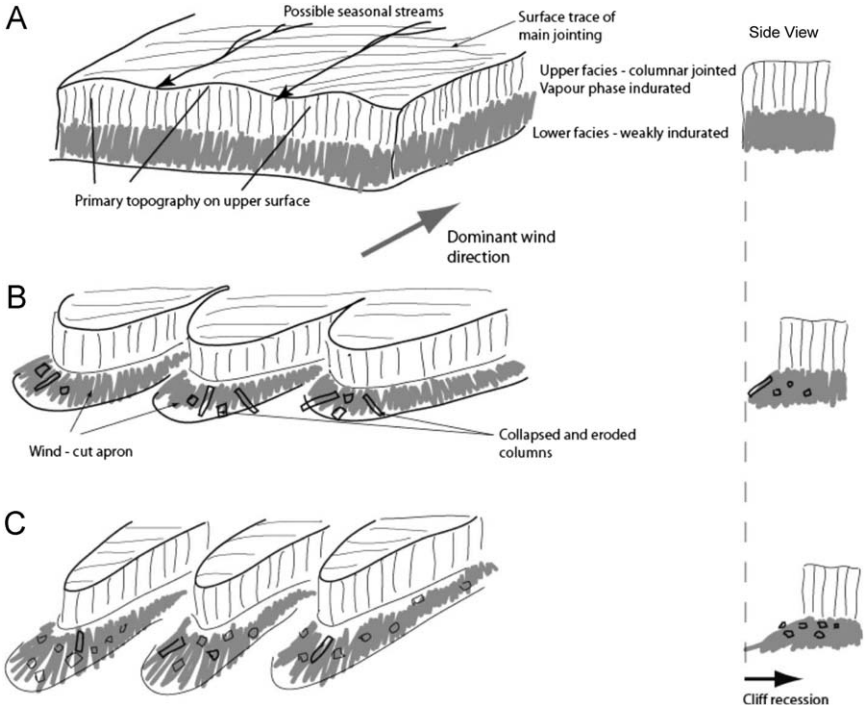

Fig. 8. Schematic depiction of the progression of megayardang formation in indurated ignimbrites. Typical association of facies in large volume ignimbrites where the upper part of the deposit is vapour-phase indurated and jointed (strong facies) while the lower part is weak and massive. (A) primary topography on sheet may be produced by fumarolic mounds, primary waves, or lobate fronts of the sheet. These may be emphasized by fluvial erosion into incipient channels. (B) The inconsistencies in the ignimbrite are exploited and accentuated by aeolian erosion that progresses with preferential erosion of the softer lower facies resulting in undercutting of the upper strong facies. The upper strong facies fails by block collapse along pervasive joints and the cliff recedes leaving a wind-cut apron of the softer facies. (C) Continuation of processes in B (undercutting, block collapse and cliff recession) results in sculpting of ignimbrite into more mature yardang forms. Serrated lateral margins of yardangs (see Fig. 7D) not shown for simplicity.

particles would be concentrated in the vortices (again abundant quartz is available as well as abundant andesite clasts) and would enhance erosion around the knobs as suggested by Whitney (1983), Greeley and Iverson (1985) and Brookes (2001). This would likely expose the lower softer layers that then would be preferentially excavated leading to a moat at the prow of the

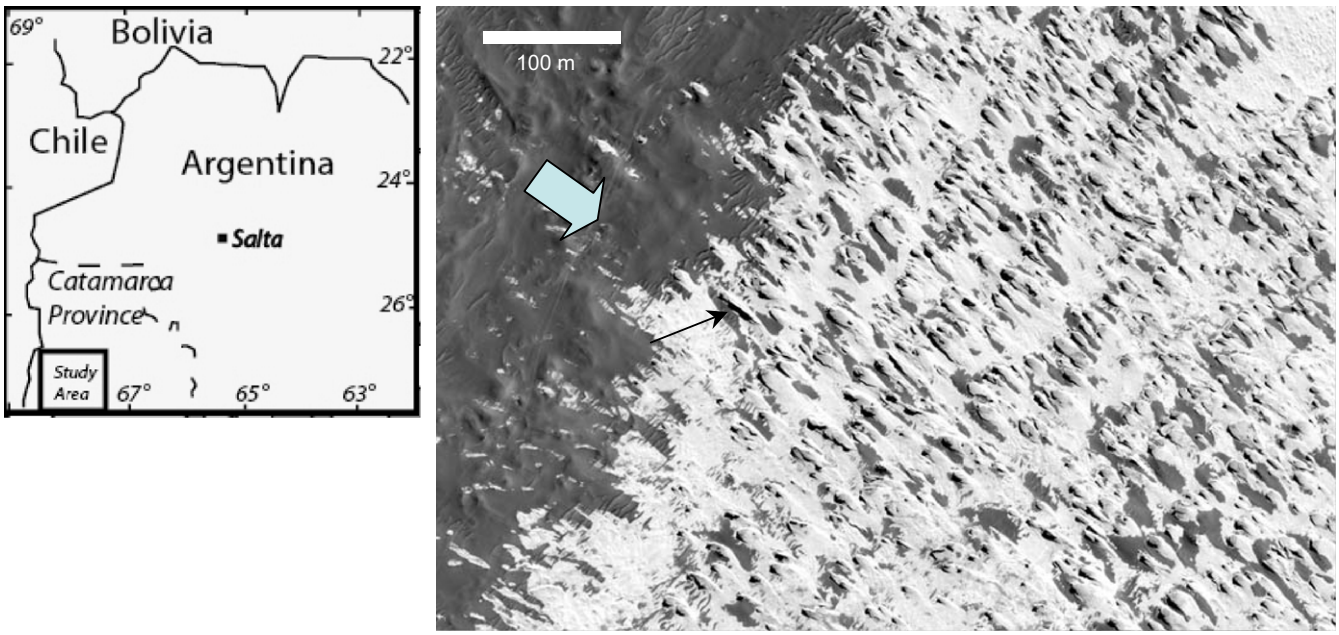

Fig. 9. Location of Campo Piedra Pomez (CPP) and aerial view of the NE corner of the study area showing the yardangs fleets of the poorly indurated ignimbrites of the CPP. Note the arrangement of the yardangs in arrays. These arrays reflect the location of fractures that are chemically indurated. Small black arrow indicated the yardang shown in Fig. 1D. Portion of GEOEYE image 08JUL16144125-P2AS-052133433010_01_ P001.

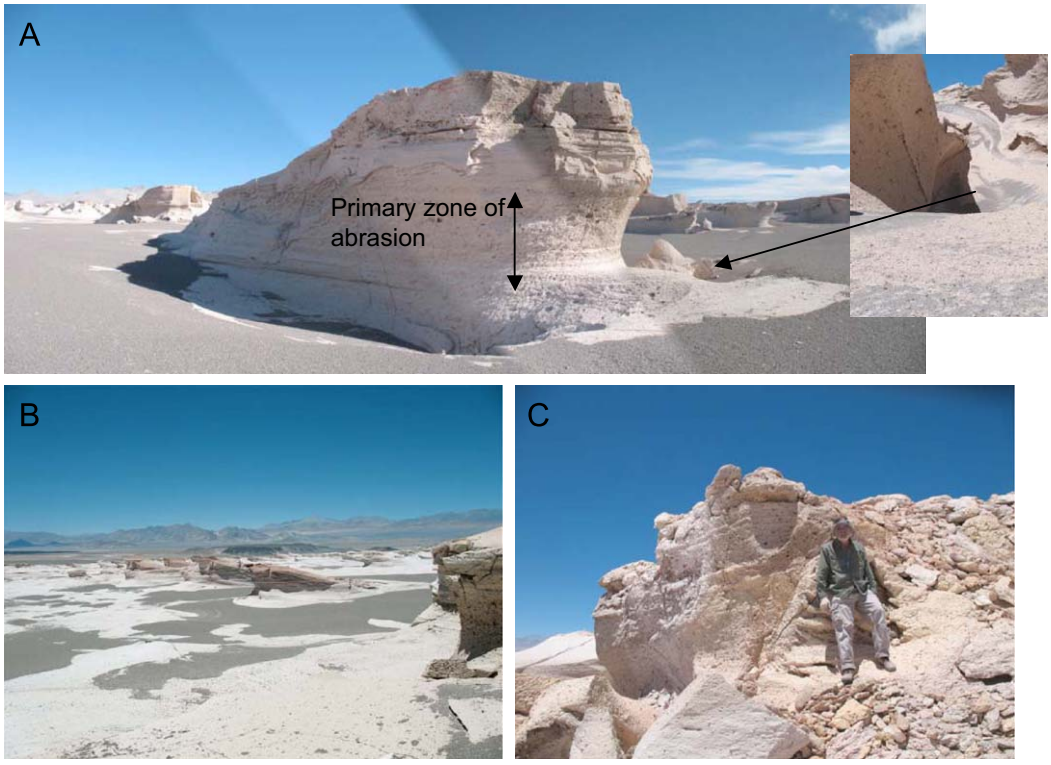

Fig. 10. Field views of yardangs in weak ignimbrites of the CPP displaying stubby forms. (A) Prow of a yardang showing the deflation hollow or moat excavated beneath the local floor. Impact of saltating quartz is the primary agent of erosion and is most effective 1–2 m above the local floor. Subsidiary currents and turbulent eddies and vortices resulting from flow separation and resulting pressure differentials results in excavation of front lateral moats that deepen and accentuate the yardang form. Block collapse is limited here but occurs elsewhere in the field (Fig. 1E). (B) A linear array of yardangs aligned along fractures that have served as pathways form hot gases that indurated the ignimbrite locally. (C) Close-up of alteration zone at the prow of the yardang. Classic "sillar" or tafoni texture produced by vapour-phase alteration and subsequent weathering is manifested by "negative" pumices and spongy appearance. This is accentuated by the wind.

yardang. The developing moat promotes further perturbation of the wind, setting up a positive feedback that results in elongation and growth of the moat and the yardang. In this case, excavation proceeds into the body of the ignimbrite beneath the local surface.

Based on the age of the ignimbrites, 70–13 ka, and heights of the yardangs we estimate that approximately 5 m of the ignimbrite thickness has been removed, yielding average erosion (vertical downcutting) rates of between 0.007 and 0.03 cm/year. We

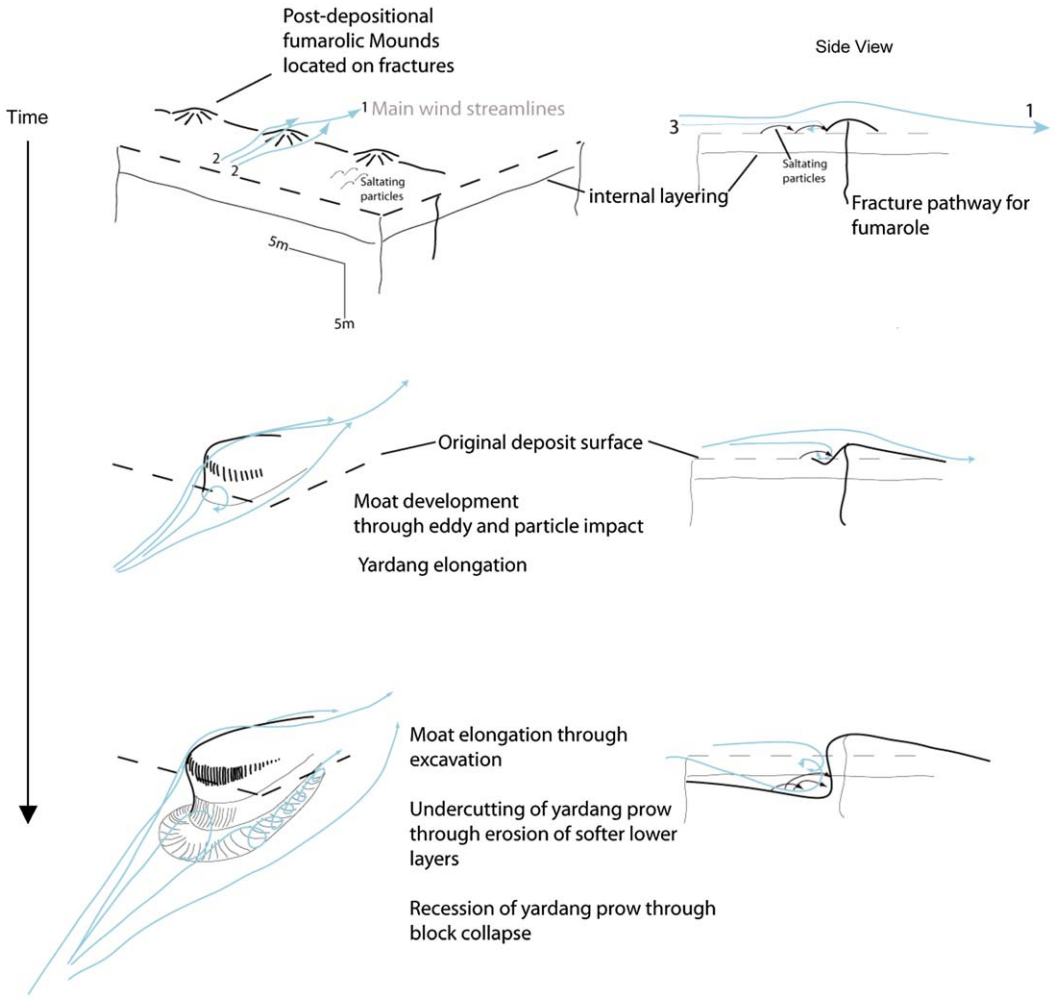

Fig. 11. Schematic showing the sequence of yardang formation in the non-indurated ignimbrites of the Campo Piedra Pomez. Here the yardangs initiate at indurated mounds or knobs on the upper surface of the sheet. Flow perturbation and saltating particles combine to erode out incipient forms that are progressively accentuated as the flow regime evolves. The moat grows in response to abrasion and excavation by saltating particles, eddies armored with impactors, and subsequent deflation by lateral flow. Side view shows progressive growth of the prow of the yardang through excavation of the deflation hollow into the ignimbrite.

hypothesize that the concave-convex form of the lower 4–6 m of the prow (Fig. 10A, B) and the depth and concavity of the moat is the result of intense vorticity (Fig. 11). The features of these small yardangs, their variably streamlined forms, with concave-convex facial associations, fluting, and keeled back slopes, and windward moats, generally support the concept of the "aerodynamic envelope" of Whitney (1983) for the development of yardangs in these weakly indurated ignimbrites. Testing of this model is planned for the future.

4. Concluding discussion

The similarity of the morphological features displayed by the megayardangs in the Medusae Fossae Formation (MFF) on Mars and those of terrestrial ignimbrites in the Altiplano Puna Volcanic Complex (APVC) in the Central Andes is striking. We find that these terrestrial megayardangs are formed when a consistent wind acts on a variably indurated lithology where an indurated layer caps a softer lower facies. Preferential erosion of the lower weak layers results in loss of support and collapse of the upper strong layers. Block collapse of the upper indurated parts and deflation of the base is the main process through which these megayardangs are sculpted, consistent with our observations from megayardangs on Mars.

Yardangs in smaller-volume, weakly indurated ignimbrites in the Campo Piedra Pomez (CPP) of the Central Andes exhibit an evolution analogous to the progression displayed in the incipient yardangs and v-shaped depressions in the MFF on Mars. These smaller or incipent yardangs in the Central Andes appear to be initiated where resistant knobs and re-entrants in the ignimbrite expose lower softer layers that are then preferentially excavated by the wind armed with saltating particles. As a windward moat develops in the softer material, a positive feedback between the growing yardang form and resulting flow separation and vortices eventually results in an aerodynamically efficient yardang form.

While the depositional processes and resulting lithologic characteristics of large ignimbrites in the Central Andes provide a viable analog to the MFF and its yardangs (Mandt et al., 2008, 2009), we recognize that large terrestrial ignimbrites are typically felsic in composition, and that large-scale silicic volcanism is not known on Mars (Francis and Woods, 1982). However, we note that basaltic ignimbrites on Earth, although considerably smaller in volume, do display similar facies variations (Freundt and Schmincke, 1995, Giordano et al. ,2006). We would anticipate that pyroclastic eruptions on Mars, even if they are mafic, would

produce deposits with a similar range of facies and therefore display physical properties similar to the large terrestrial ignimbrites discussed here.

Ultimately, our observations are not necessarily lithology-specific. We ratify the importance of strong unidirectional winds and recognize the importance of indurated lithologies as the primary factors in megayardang formation. Different degrees and distribution of induration will produce different forms of yardangs. Our observations are supported by the limited experimental data on erosion of yardangs. These experiments showed that yardang formation in models with hard layers-over-soft progressed by undercutting, collapse and rapid deflation, whereas soft-over-hard developed blunt heads and broad wide convex backs (e.g. McCauley et al., 1977a, Ward and Greeley, 1984). Our observation of an evolving erosional moat trough at the prow of the yardang in the weaker ignimbrites has no experimental analog and may implicate a more prominent role for vorticity in the development of some yardangs. Finally, jointing, which is ubiquitous in indurated ignimbrites, does not play a primary role in yardang orientation, but can facilitate sculpting of the yardang. Where prominent jointing is oblique to yardang orientation and deposit edges, serrated margins like those seen in the MFF on Mars may develop.

Acknowledgements

Support for work on Andean ignimbrites is funded by the National Science Foundation and support from the Oregon Space Grant Consortium has allowed de Silva to develop and conduct this analog research. J.G. Viramonte wishes to thank the Ministerio de Ciencia y Técnica, Argentina, Grant PICT 07-38131 for support the field work in the Cerro Blanco Caldera Complex. The comments of two anonymous journal reviewers have helped clarify our focus and presentation considerably. This paper is dedicated to the memory of Peter Francis, who first introduced SdeS to yardangs.

References

Allmendinger, R.W., Jordan, T.E., Kay, S.M., Isacks, B.L., 1997. The evolution of the Altiplano–Puna plateau of the Central Andes. Annual Reviews of Earth and Planetary Sciences 25, 139–174.

Arnosio, M., Becchio, R., Viramonte, J., Groppelli, G., Norini, G., and Corazzato, C., 2005, Geología del complejo volcánico Cerro Blanco (26° 45'S–67° 45'W), Puna Austral. In: Proceedings of the XVI Congreso Geológico Argentino, vol. 1, pp. 851–855.

Bailey, J.E., Self, S., Wooller, L.K., Mouginis-Mark, P.J., 2007. Discrimination of fluvial and eolian features on large ignimbrite sheets around La Pacana Caldera, Chile, using Landsat and SRTM-derived DEM. Remote Sensing of Environment 108 (1), 24–41.

Blackwelder, E., 1934. Yardangs. Bulletin of the Geological Society of America 45, 159–166.

Bradley, B.A., Sakimoto, S.E.H., Frey, H., Zimbelman, J.R., 2002. Medusae Fossae formation: new perspectives from Mars Global Surveyor. Journal of Geophysical Research 107 (E8), 2.1–2.17.

Branney, M.J., Kokelaar, B.P., 2002. Pyroclastic density currents and the sedimentation of ignimbrites. Geological Society London Memoir 27, 143.

Breed, C.S., J.F. McCauley and M.I. Whitney, 1989. Wind erosion forms. In: Thomas D.S.G. (Ed.), Arid Zone Geomorphology, Belhaven Press (London) and Halsted Press (Toronto), pp. 284–307.

Brookes, I.A., 2001. Aeolian erosional lineations in the Libyan Desert, Dakhla Region, Egypt. Geomorphology 39, 189–209.

Cas, R.A.F. and J.V. Wright, 1992.Volcanic Successions, Modern and Ancient: A Geological Approach to Processes, Products and Successions, Chapman & Hall (London, New York).

Crown, D.A., R. Greeley, M.F. Sheridan, and R. Carrasco, 1989. Analysis of an ignimbrite plateau in the Central Andes using LANDSAT thematic mapper data: implications for the identification of ash deposits on Mars (Abstract). Proceedings of the Lunar and Planetary Science Conference, XX, 207.

Das, D.K., Jarratt, D., McDonald, D., Heberlein, D., 1998. Environmental Baseline Data Collection at Diablillos Property, Salta, Argentina. Rescan Environmental Services and Barrick Exploraciones Argentina S.A., 15 pp.

de Silva, S.L., 1989aa. Geochronology and stratigraphy of the ignimbrites from the 21° 30'S to 23° 30'S portion of the Central Andes of N. Chile. Journal of Volcanology and Geothermal Research 37 (2), 93–131.

de Silva, S.L., 1989bb. The Altiplano–Puna volcanic complex of the Central Andes. Geology 73 (12), 1102–1106.

de Silva, S.L., Zandt, G., Trumbull, R., Viramonte, J., Salas, G., Jimenez, N., 2006. Large-scale silicic volcanism in the Central Andes—a tectonomagmatic phenomenon. In: de Natale, G., Troise, C., Kilburn, C. (Eds.), Mechanisms of Activity and Unrests at Large Calderas. Special Publication 269 by Geological Society of London, pp. 47–64.

de Silva, S.L. , Bailey, J.E., and Mandt, K.E., 2008. Aeolian erosion of terrestrial ignimbrites and the formation of yardangs: synergistic remote and field observations on Earth with applications to Mars (Abstract). Eos Transactions of the American Geophysical Union 89(53), Fall Meeting Supplement, H21C-2117.

Forsythe, R.D., Zimbelman, J.R., 1988. Is the Gordii Dorsum escarpment on Mars an exhumed transcurrent fault?. Nature 336 (6195), 143–146.

Francis, P.W., Wood, C.A., 1982. Absence of silicic volcanism on Mars: implications for crustal composition and volatile abundance. Journal of Geophysical Research 87 (B12), 9881–9889.

Freundt, A., Schmincke, H.-U., 1995. Eruption and emplacement of basaltic welded ignimbrite during caldera formation on Gran Canaria. Bulletin of Volcanology 56, 640–659.

Gaupp, R., Kött, A., Wörner, G., 1999. Palaeoclimatic implications of Mio-Pliocene sedimentation in the high-latitude intra-arc Lauca basin of northern Chile. Palaeogeography, Palaeoclimatology, Palaeoecology 151, 79–100.

Giordano, G., De Benedetti, A.A., Diana, A., Diano, G., Gaudioso, F., Marasco, F., Miceli, M., Mollo, S., Cas, R.A.F., Funicello, R., 2006. The Colli Albani mafic cladera (Roma, Italy): stratigraphy, structure, and petrology. Journal of Volcanology and Geothermal Research 155, 49–80.

Goudie, A.S., 2007. Mega-Yardangs: a global analysis. Geography Compass 1 (1), 65–81.

Greeley, R., and J.E. Guest, 1987.Geologic map of the eastern equatorial region of Mars. US Geological Survey Miscellaneous Investigations Series Map, I-1802-B. US Geological Survey, Washington, DC.

Greeley, R., Iverson, J.D., 1985. Wind as a Geological Process on Earth, Mars, Venus and Titan. Cambridge University Press 333..

Greene, L.L., 1995. Eolian landforms in the Central Andes: implications for the long-term stability of atmospheric circulation. Unpublished M.S. Thesis, Cornell University, Ithaca, 62 pp.

Guest, J.E., 1969. Upper Tertiary ignimbrites in the Andean Cordillera of part of the Antofagasta province of northern Chile. Geological Society of America Bulletin 80, 337–362.

Hartley, A.J., Guillermo Chong, G., 2002. Late Pliocene age for the Atacama Desert: implications for the desertification of western South America. Geology 30, 43–46.

Head, J.W., and M.A. Kreslavsky, 2004. Medusae Fossae Formation: ice-rich airborne dust deposited during periods of high obliquity? (Abstract). In: Proceedings of the 35th Lunar Planet. Science Conference, No. 1635.

Hynek, B.M., Phillips, R.J., Arvidson, R.E., 2003. Explosive volcanism in the Tharsis region: global evidence in the Martian geologic record. Journal of Geophysical Research 108 (E9), 15.1–15.16.

Inbar, M., Risso, C., 2001. Holocene yardangs in volcanic terrains in the southern Andes, Argentina. Earth Surface Processes and Landforms 26, 657–666.

Malin, M.C., Edgett, K.S., 2000. Sedimentary rocks of early Mars. Science 290 (5498), 1927–1937.

Mandt, K., de Silva, S.L., Zimbleman, J., Crown, D.A., 2008. The origin of the Medusae Fossae Formation, Mars: insights from a synoptic approach. Journal of Geohysical Research (Planets) 113 (E12011 doi:10.1029/2008JE003076.

Mandt, K., de Silva, S.L., Zimbelman, J., and Wyrick, D., 2009. Distinct erosional progressions in the Medusae Fossae Formation, Mars, indicate contrasting environmental conditions. Icarus, 10.1016/j.icarus.2009.06.031.

McCauley, J.F., 1973. Mariner 9 evidence for wind erosion in the equatorial and mid-latitude regions of Mars. Journal of Geophysical Research 78, 4123–4137.

McCauley, J.F., Grolier, M.J., Breed, C.S., 1977aa. Yardangs of Peru and other desert regions. USGS, Interagency Report, Astrogeology 81, 177.

McCauley J.F., C.S. Breed, and M.J. Grolier, 1977b. Yardangs. In: Doehring, D.O. (Ed.), Geomorphology in Arid Regions, Eighth Annual Geomorphology Symposium, Binghampton, NY. Allen and Unwin, Boston, pp. 233–269.

Mouginis-Mark, P., 1993. The influence of oceans on martian volcanism (Abstract). In: Proceedings of the 24th Lunar and Planetary Science Conference, pp. 1021–1022.

Nussbaumer, J., 2005. Extent and further characteristics of former glaciated terrain in Elysium Planitia, Mars (Abstract). In: Proceedings of the 36th Lunar and Planetary Science Conference, p. 1949.

Parker, T.J., 1991. A comparison of the Martian Medusae Fossae Formation with terrestrial carbonate platforms (Abstract). In: Proceedings of the 22nd Lunar and Planetary Science Conference, pp. 1029–1030.

Richards, J.P., Villeneuve, M., 2002. Characteristics of late Cenozoic volcanism along the Archibarca lineament from Cerro Llullaillaco to Corrida de Cori, northwest Argentina. Journal of Volcanology and Geothermal Research 116, 161–200.

Roever, W.P.D.E., 1966. Dacitic ignimbrites with upward increasing compactness near Sibolangit (NE Sumatra, Indonesia) and their peculiar hydrology. Bulletin Volcanologique 29, 105.

Ross, C.S., Smith, R.L., 1961. Ash-flow tuffs—their origin, geologic relations, and identification. US Geological Survey Professional Paper 366, 81.

Schultz, P.H., Lutz, A.B., 1988. Polar wandering on Mars. Icarus 73, 91–141.
Scott, D.H., Tanaka, K.L., 1982. Ignimbrites of Amazonis Planitia region of Mars. Journal of Geophysical Research 87, 1179–1190.
Scott, D.H., and K.L. Tanaka, 1986. Geologic map of the western equatorial region of Mars, US Geological Survey Miscellaneous Investigations Series Map, I-1802-A. US Geological Survey, Washington, DC.
Selby, M.J., Augustinus, P., Moon, V.G., Stevenson, R.J., 1988. Slopes on strong rock masses: modeling and influences of stress distribution and geomechanical properties. In: Anderson, M.G. (Ed.), Modelling Geomorphological Systems. Wiley and Sons, pp. 341–374.
Tanaka, K.L., 2000. Dust and ice deposition in the Martian geologic record. Icarus 144, 254–266.
Ward, A.W., 1979. Yardangs on Mars: evidence of recent wind erosion. Journal of Geophysical Research 84, 8147–8166.
Ward, A.W., Greeley, R., 1984. Evolution of Yardangs at Roger Lake, California. Geological Society of America Bulletin 95, 829–837.
Whitney, M.I., 1983. Eolian feature shaped by aerodynamic and voricity processes. In: Brookfield, M.E., Ahlbrandt, T.S. (Eds.), Eolian Sediments and Processes. Elseivier, Amsterdam, pp. 223–245.